Supplementary Information for: "The Economics of Firm Solar Power From Li-ion and Vanadium Flow Batteries in California"

Diarmid Roberts[1*] and Solomon Brown[1]

[1*]Department of Chemical and Biological Engineering, The University of Sheffield, Mappin St., Sheffield, S1 4NL, South Yorkshire, United Kingdom.

*Corresponding author(s). E-mail(s): d.roberts1@sheffield.ac.uk;
Contributing authors: s.f.brown@sheffield.ac.uk;

1 VFB Bottom up Price Model

This model is based on the ones reported in [1] and [2], with minor adjustments to the treatment of the pumping requirements. The stack area A (m^2) of the VFB is defined by:

$$A = \frac{1000 P_{Inv.}}{\bar{I}^d OCV_{50\%} \sqrt{\eta_V}(1 - l_{BOP})\sqrt{\eta_{Inv.}}} \tag{1}$$

where $P_{Inv.}$ is the inverter rating defining the maximum BESS output (kW), $\bar{I}^d$ is the maximum discharge current density (A/m^2), $OCV_{50\%}$ the open cell voltage at 50% SOC, η_V the round-trip voltaic efficiency, and $\eta_{Inv.}$ the round trip inverter efficiency.

The maximum flow rate (and hence pump rating, L/s) for the catholyte is determined by:

$$Q_+^{max} = \frac{A\bar{I}^d r_{flow}}{C_+ min(SOC_{min}, 1 - SOC_{max}, \delta_{SOC})\sqrt{\eta_C}} \tag{2}$$

where r_{flow}, the ratio describing the over-supply of electrolyte flow to avoid diffusion limitations is added following the experimental details in [3]. SOC_{min}

is the lowest permitted SOC, SOC_{max} the highest, δ_{SOC} the maximum permitted change in SOC through the cell per pass, η_C the coulombic efficiency and C_+ the coulombic concentration (C/L) of the catholyte, defined as:

$$C_+ = \frac{n_e F c_+}{s_+} \tag{3}$$

where n_e, the number of electrons transferred in the redox reaction and s_+, the number of species participating in the reaction (stoichiometry) are both 1. F is the Faraday constant (96 485 C/mol) and c_+ is the concentration of the catholyte redox active species (mol/L).

The presence of η_C on the denominator in 2 ensures sufficient charge is supplied in chemical form to cover the coulombic losses due to active species crossover and shunt currents.

The inclusion of the minimum of SOC_{min}, SOC_{max} and δ_{SOC} on the denominator of 2 adds a level of stringency above that of Viswanathan *et al.*, who applied only the SOC_{min}. This reflects the fact that active species depletion during charging, and the need to maintain a maximum drop in SOC across the stack can also lead to inflation of the required flow rate.

The calculation shown in 2 is repeated for the anolyte flow $Q_{-,max}$ using c_- and s_-.

The inventory of catholyte species (mol) required to satisfy one hour of discharge is then defined by:

$$m_+ = \frac{3.6\text{e}6 P_{Inv.} c_+}{OCV_{50\%}(SOC_{max} - SOC_{min})C_+} \tag{4}$$

The inventory of each supporting counter ion species (mol) may be calculated for the catholyte by:

$$m_{CI,+,n} = \frac{m_+ c_{CI,+,n}}{c_+} \tag{5}$$

where $c_{CI,+,n}$ is the concentration of the n^{th} counter ion (allowing for mixed acid electrolytes) in the catholyte. An analogous calculation is performed for the anolyte. In the case of the VFB it is assumed that the concentrations of counter ions are the same on both sides of the membrane.

The volume of storage required for the catholyte (L) was calculated by:

$$V_+ = \frac{m_+}{c_+} \tag{6}$$

an analagous calculation was used for the anolyte.

The total price of the power basis components is then defined by:

$$price_{kW} = A \cdot price_{areal} + (Q_+ + Q_-) price_{Pump} + price_{HEX} + UPLM \tag{7}$$

where $price_{pump}$ is the pump price ($s/L). Ha and Gallagher used a bottom up model to estimate the "Unit Price Less Materials" (UPLM) for a VFB

with a 5 h duration, and compared this to that of a LIB with the same specification (using the Argonne BatPac model for the latter) [4]. It is assumed that the UPLM will scale with power rating, as the article mentions number of stacks per year as the scale. For a given capacity output per annum, they report a lower UPLM for the VFB, attributed to the higher current density of the latter and the resultant lower area specific costs. The current density assumed by Ha and Gallagher (approx 190 mA/cm^2) for the VFB is similar to that of the VFB in the present base case scenario (219 mA/cm^2), so the stack manufacturing requirements captured in the UPLM should be appropriate. The area specific price $price_{areal}$ ($\$1/m^2$) is defined according to the cell components representing a repeating unit in a stack by:

$$price_{areal} = price_{Memb.} + 2price_{CE} + price_{BPP} + price_{areal,other} \quad (8)$$

where the terms on the right hand side represent, respectively, the cost of the membrane/separator, the carbon felt electrodes and the bipolar plate.

In this model the cost of end plates is ignored, as these would represent a small fraction of the cost for a 105 V stack (the voltage considered in [4]).

The total price of components on an energy basis are then calculated by:

$$price_{kWh} = ((m_{+} \cdot price_{+} + m_{-} \cdot price_{-} + \sum_{n} m_{CI,n} \cdot price_{CI,n}) \cdot MC_E + (V_{+} + V_{-}) price_{tank}) P$$

(9)

where $price_{+}$ and $prices_{-}$ are the prices of the redox active species in the catholyte and anolyte respectively, $price_{CI,n}$ the price of the nth supporting species (all in \$1/mol), MC_E the electrolyte manufacturer cost factor (e.g. 1.1 for 10%) and $price_{tank}$ the price of chemical storage (\$1/L). As the UPLM parameter is assumed to scale with power, the energy component prices are multiplied by PM_{RFB}, an assumed profit margin factor for the RFB manufacturer. It is assumed that the electrolyte is manufactured by the same entity that manufactures the RFB. If this were not the case, an additional profit margin would need to be applied to the total electrolyte cost.

1.0.1 Base Scenario VFB Parameters

The approach to price model parametrisation for the base case VFB was to collect as much recent data from the literature as possible, and generate average values for present day and future scenarios. This task was aided by the recent review of Minke and Turek which collated cost data for key stack components [5]. For the data taken from Viswanathan *et al.*, "Near term" was used for the present case, as this shows better agreement with other sources than the "Present" values do [2]. Nafion NR212 is used as the membrane in the modelB, as this material was used in the system from which performance parameters are drawn [3]. Although potentially cheaper due to the reduced

material requirements, the thinner Nafion NR211 did not show improved performance, and was described as being difficult to handle [6]. As the sources tend to use "cost", a profit margin of 12% is applied to each component in order to avoid underestimating the VFB manufacturer's costs [7]. The data obtained are shown in 1

Table 1 VFB Component Price Parameters. *Present/future.

Scaling	Component	Cost unit	Cost*	$ exchg.	PM	Price*	Source
1/kW	Nafion NR212		301/48	1.10		370/59	[5]
	Bipolar Plate	€ $1/m^2$	100/50	1.10		123/62	[5]
	Felt electrode		53/16	1.10	12%	65/20	[5]
	Other Area Specific*	$1/m^2$	8/3	1		9/3	[1, 2]
	Pump	$s/L		1		500/400	[3]
	HEX	$1/kW	56/37	1		63/41	[2]
	UPLM	$1/kW		1		173/158	[4]
$1/(kW h)	V	$1/mol		1		1.55/1.55	[8]
	HCl	$1/mol		1		0.021/0.021	[9]
	H_2SO_4	$1/mol		1		0.020/0.020	[10]
	MC_E					10%	[11]
	Tank (HDPE)	$1/L	0.09/0.08	1		0.10/0.09	[2]
	PM_{RFB}					10%	Estimate

Other area specific costs is the average of those given in the two sources. Under pump costs, a figure of $900 s/L was reported in [12] for an acid compatible unit. This cost is higher than the current price of the pump used in the VFB reported by [3]. According to the brochure, that pump is capable of 1.25 L/s at the base case stack pressure drop of 0.34 bar [13]. At the time of writing, this pump is available in the US for a price of $ 500, giving a pump price of $400 s/L. The large discrepancy between the two sources may be explained by the former source being 7 years old. For this reason, the Reed pump price is used for the present scenario, but a 25% contingency is added in case custom seal arrangements are necessary. For the future scenario, a price decrease of 20% is estimated to be achieved by volume discounting.

The inclusion of a price for a heat exchanger (HEX) is conservative. The mixed acid electrolyte used in the Reed system allows a higher electrolyte temperature to be reached before precipitation occurs, and in principle this will allow greater passive cooling [14]. Viswanathan *et al.* factored this in their cost estimates for sulphuric acid and mixed acid systems, removing the heat exchange cost component from the latter [2]. However the ability to operate without a heat exchanger is merely asserted, and a detailed study of the thermal management has not been carried out to the best of the author's knowledge. HEX is assumed to be a VFB specific component of the DC module cost, and it is assumed that more generic heat management equipment required at the container level is included in the BOSH figure defined in [15].

Future cost decreases are primarily attributed to economies of scale. Where the manufacturing scale scope of the study is stated, present day estimates are

associated with a scale of <300 MW and future scenarios with 1 GW - 2 GW [1, 2, 4].

A vanadium price of $1.55/mol is derived from a vanadium pentoxide price of $17/kg, this being the average European spot price from January 2006 to April 2020 (data are assumed to have been corrected to 2020 $) [8]. Predicting a future price for vanadium is beyond the scope of this project hence the same price is assumed for the future scenario. A price of $ 200 per wet ton for industry grade 35% HCl was used, based on prices shown on a Chinese commodity purchasing platform at the time of writing [9]. This price is assumed to include a shipping component, as prices at factory are typically considerably lower [16]. A price of $200 per ton was also used for 98% industrial grade H_2SO_4 [10].

Minke and Turek mention reducing agents and additives as additional cost components in the electrolyte manufacture but do not report 1/(kW h) estimates for these [5]. The PNNL system used to parametrise this model did not include additives according to the experimental description, hence these are ignored. It is likely in any case that the contribution would be small relative to that of vanadium.

The performance parameters for the VFB are predominantly taken from the system reported by Reed *et al.* in 2016 [3], except δ_{SOC} and l_{BOP} where a more generic approach is taken. Reed *et al.* tested various electrode flow architectures on a 1 kW VFB stack based on a 50 µm Nafion NR212 membrane. In the base case scenario, performance data are taken from the test of the highest performing stack architecture (IDD2s) at an electrolyte flow rate of 400 mL/min per cell. This setup was tested at three current-densities: 160, 240 and 320 mA/cm^2. At each test condition efficiency data were obtained as integrals over a cycle between 15% and 85% SOC.

In the parametrisation of the VFB for the base case scenario the target for η_{DC} was fixed at 0.75. A coulombic efficiency (η_C) of 0.975 was derived as the average of the values reported by [3] at the three current-densities tested, which only varied between 0.974 and 0.976. For the base case system the η_{DC} requirement is satisfied when the voltaic efficiency η_V is 0.801, which corresponds (by linear interpolation) to a current-density ($\bar{I}^d$) of 219 mA/cm^2. $OCV_{50\%}$ was taken from a linear best fit line of data in [14], where the OCV of a chloride electrolyte was reported at 20%, 50% and 80% SOC. Although a different electrolyte, based on a mixture of sulphuric acid and hydrochloric acid, was used in [3] the OCV data were not published.

2 summarises the technical parameter values representing the VFB in the bottom up price model.

The flow over-supply ratio r_{flow} was estimated by analysis of the experimental details in [3]. At the lowest permitted SOC during discharge, the concentration of unreacted vanadium would be 0.3 mol. At the flow rate of 400/min, a current of 193 A passes through each cell in chemical form [1]. The

[1] It is assumed that this flow rate is used on both sides of the membrane, otherwise the flow would be insufficient

Table 2 Parameters describing base scenario VFB in the pricing model.

Parameter	Value	Units	Source
η_{DC}	0.75	-	Set
$\eta_{Inv.}$	0.96	-	[17]
η_V	0.801	-	
η_C	0.975	-	
$\bar{I}^d$	219	mA/cm^2	
SOC_{min}	0.15	-	
SOC_{max}	0.85	-	[3]
c_+, c_-	2	M	
c_{HCL}	5	M	
$c_{H_2SO_4}$	2	M	
r_{flow}	1.12	-	
δ_{SOC}	0.2		[12]
$OCV_{50\%}$	1.47	V	[14]
l_{BOP}	0.02	-	[1, 18, 19]

current required at the electrode is calculated as the product of I_{rated} and the cell area divided by the one way coulombic efficiency. For the reported cell area of 780 cm^2 this figure is 173 A, hence the flow over supply is 12%.

An estimate for l_{BOP} is obtained by averaging the three sources. In [19] a 2.3% round trip pumping loss is interpreted here as a one way loss of 1.1%. The shunt current losses reported (1.1% round trip) are ignored, because in the Reed system these will be accounted for in the coulombic efficiency term. The figure in [1] is a generic estimate given in the form of charge/discharge system efficiencies of 0.94, giving l_{BOP} of 6%. However, this includes PCS losses, which in this study are included at a one way value of 2%. To avoid double counting, this loss and the one way figure for the shunt loss in [19] are subtracted from this figure to give 3.4%. In [18] a pumping power of 20 W is required at the maximum flow rate tested for a 1.1 kW stack, giving a figure of 1.8%.

2 Efficiency Assumptions

Literature data on internal resistances for an NMC cell similar to the one tested by Schmalstieg *et al.* [20] were obtained from an experimental study [21], summed and used to calculate the round trip efficiency at various C-rates using a basic I^2R model, as shown in 1. In doing this, it is assumed that, unlike in the VFB, there are no fixed losses associated with the LIB system at the DC boundary, and that the coulombic efficiency is 100%.

Initial scoping work for the case study showed that the optimal duration for self-sufficiency from PV is greater than 4 h, hence the maximum C rate possible is 1/4. Therefore, 0.98 is a good approximation for the DC efficiency of the LIB. This figure was multiplied by an assumed constant round trip inverter efficiency of 0.96 to obtain the 0.94 value used in the study. This value is very similar to the 0.95 applied by [22].

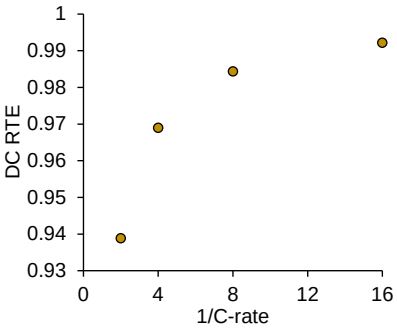

Fig. 1 Approximation of DC round trip efficiency for a 2.6 A h Li-ion cell using a quadratic model.

For the VFB, where the efficiency varies more strongly with current, the model reported in [23] was applied to estimate the variation in AC efficiency with current-density, as shown in 2.

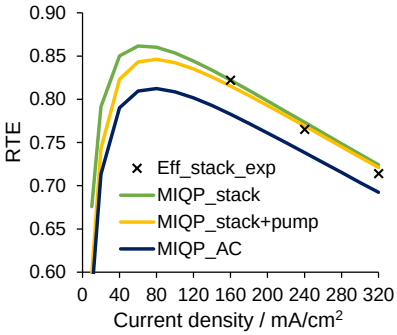

Fig. 2 A comparison of experimental round trip stack energy efficiency data from the IDD2s PNNL system in [3] with the MIQP model output. Note that the VFB in the case study is specified to have a maximum current density of 219 mA/cm^2 corresponding to an AC efficiency of 0.75.

By applying this model to the scheduling of VFB in the firm PV case study, it was found that the predicted operational AC efficiency was near constant at around 0.80 across the studied range of SSR scenarios. This is due to the asymmetry of the charge/discharge requirement, with discharging typically occurring at a lower fraction of the rated power. As the power rating of the VFB is increased to provide higher SSR, a drop in the discharge efficiency due to moving below the optimal current density seen in 2 is countered by a gain in efficiency on the charging side as the current-density moves back toward the peak efficiency point. The 0.78 figure used in the case study hence contains a contingency in case of increased shunt currents at the full stack scale, or over-optimistic assumptions about pump efficiency.

Both LIB and VFB will likely suffer from additional parasitic losses not accounted for in the model, but these are assumed to be similar for both systems.

3 Temperature Data

In the base scenario the temperature data were For temperature, it is assumed that the LIB is stored outdoors, not air conditioned, and hence the cell temperature tracks the ambient temperature. Two sets of hourly data from 2012 were downloaded from [24]. The San Diego site is coastal, whereas the March Air Reserve Base site is inland. These are shown in 3 and 4.

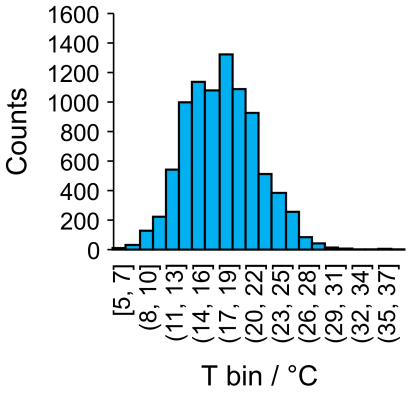

Fig. 3 Hourly 2012 temperature data from the weather station at San Diego International Airport

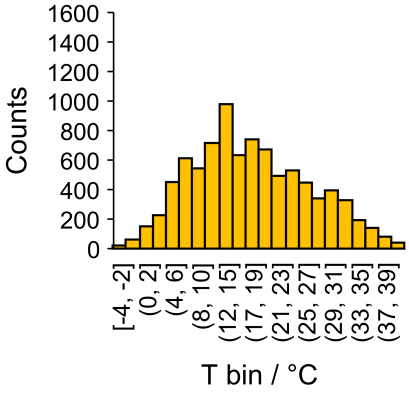

Fig. 4 Hourly 2012 temperature data from the weather station at March Air Reserve Base

The two sets have the same annual average of 17.5 °C, but the former has a narrower range due to the coastal location.

References

[1] Darling, R.M., Gallagher, K.G., Kowalski, J.A., Ha, S., Brushett, F.R.: Pathways to low-cost electrochemical energy storage: a comparison of aqueous and nonaqueous flow batteries. Energy Environ. Sci. **7**(11), 3459–3477 (2014). https://doi.org/10.1039/C4EE02158D

[2] Viswanathan, V., Crawford, A., Stephenson, D., Kim, S., Wang, W., Li, B., Coffey, G., Thomsen, E., Graff, G., Balducci, P., Kintner-Meyer, M., Sprenkle, V.: Cost and performance model for redox flow batteries. Journal of Power Sources **247**, 1040–1051 (2014). https://doi.org/10.1016/j.jpowsour.2012.12.023

[3] Reed, D., Thomsen, E., Li, B., Wang, W., Nie, Z., Koeppel, B., Kizewski, J., Sprenkle, V.: Stack Developments in a kW Class All Vanadium Mixed Acid Redox Flow Battery at the Pacific Northwest National Laboratory. Journal of The Electrochemical Society **163**(1), 5211–5219 (2016). https://doi.org/10.1149/2.0281601jes

[4] Ha, S., Gallagher, K.G.: Estimating the system price of redox flow batteries for grid storage. Journal of Power Sources **296**, 122–132 (2015). https://doi.org/10.1016/j.jpowsour.2015.07.004

[5] Minke, C., Turek, T.: Materials, system designs and modelling approaches in techno-economic assessment of all-vanadium redox flow batteries – A review. Journal of Power Sources **376**, 66–81 (2018). https://doi.org/10.1016/j.jpowsour.2017.11.058

[6] Reed, D., Thomsen, E., Wang, W., Nie, Z., Li, B., Wei, X., Koeppel, B., Sprenkle, V.: Performance of Nafion® N115, Nafion® NR-212, and Nafion® NR-211 in a 1 kW class all vanadium mixed acid redox flow battery. Journal of Power Sources **285**, 425–430 (2015). https://doi.org/10.1016/j.jpowsour.2015.03.099

[7] Investopedia: Which segments of the chemical sector have the highest profit margins? https://www.investopedia.com/ask/answers/060115/which-segments-chemicals-sector-have-highest-profit-margins.asp Accessed 2020-05-08

[8] Live Vanadium Price, News and Articles. https://www.vanadiumprice.com/ Accessed 2018-08-23

[9] AliBaba https://www.alibaba.com/showroom/bulk-hydrochloric-acid.html Accessed 2020-05-14

[10] AliBaba https://www.alibaba.com/showroom/bulk-sulphuric-acid.html Accessed 2020-05-14

[11] Eckroad, S.: Vanadium Redox Flow Batteries: An In-Depth Analysis. Technical Report 3, The Electric Power Research Institute (2007). https://doi.org/10.1039/c3cp52035h. http://www.paredox.com/foswiki/pub/Trash/TrashAttachment/EPRI_-_Vanadium_Redox_Flow_Batteries_2007_.pdf

[12] Cho, K.T., Albertus, P., Battaglia, V., Kojic, A., Srinivasan, V., Weber, A.Z.: Optimization and Analysis of High-Power Hydrogen/Bromine-Flow Batteries for Grid-Scale Energy Storage. Energy Technology **1**(10), 596–608 (2013). https://doi.org/10.1002/ente.201300108

[13] PREMIUM MAGNETIC-DRIVE SEALLESS CENTRIFUGAL PUMPS DB & SP SERIES. https://voigtabstore.com/content/DB/brochure.pdf Accessed 2020-05-18

[14] Kim, S., Vijayakumar, M., Wang, W., Zhang, J., Chen, B., Nie, Z., Chen, F., Hu, J., Li, L., Yang, Z.: Chloride supporting electrolytes for all-vanadium redox flow batteries. Physical Chemistry Chemical Physics **13**(40), 18186 (2011). https://doi.org/10.1039/c1cp22638j

[15] Roberts, D., Brown, S.: DC to turnkey: An analysis of the balance of costs for behind the meter BESS at commercial/industrial sites. Energy Reports **7**, 20–23 (2021). https://doi.org/10.1016/j.egyr.2021.02.060

[16] Bowen, B. https://www.icis.com/explore/resources/news/2017/06/08/10114252/us-hydrochloric-acid-prices-jump-higher-on-outages/ Accessed 2020-05-14

[17] Mongird, K., Fotedar, V., Viswanathan, V., Koritarov, V., Balducci, P., Hadjerioua, B., Alam, J.: Energy storage technology and cost characterization report. Technical Report PNNL-28866, Pacific Northwest National Laboratory (2019)

[18] Kim, S., Thomsen, E., Xia, G., Nie, Z., Bao, J., Recknagle, K., Wang, W., Viswanathan, V., Luo, Q., Wei, X., Crawford, A., Coffey, G., Maupin, G., Sprenkle, V.: 1 kW/1 kWh advanced vanadium redox flow battery utilizing mixed acid electrolytes. Journal of Power Sources **237**, 300–309 (2013). https://doi.org/10.1016/j.jpowsour.2013.02.045

[19] Crawford, A., Viswanathan, V., Stephenson, D., Wang, W., Thomsen, E., Reed, D., Li, B., Balducci, P., Kintner-Meyer, M., Sprenkle, V.: Comparative analysis for various redox flow batteries chemistries using a cost performance model. Journal of Power Sources **293**, 388–399 (2015). https://doi.org/10.1016/j.jpowsour.2015.05.066

[20] Schmalstieg, J., Käbitz, S., Ecker, M., Sauer, D.U.: A holistic aging model for Li(NiMnCo)O2 based 18650 lithium-ion batteries. Journal of Power Sources **257**, 325–334 (2014). https://doi.org/10.1016/j.jpowsour.2014.02.012

[21] Muenzel, V., Hollenkamp, A.F., Bhatt, A.I., De Hoog, J., Brazil, M., Thomas, D.A., Mareels, I.: A comparative testing study of commercial 18650-format lithium-ion battery cells. Journal of the Electrochemical Society **162**(8), 1592–1600 (2015). https://doi.org/10.1149/2.0721508jes

[22] Fisher, M., Apt, J., Whitacre, J.F.: Can flow batteries scale in the behind-the-meter commercial and industrial market? A techno-economic comparison of storage technologies in California. Journal of Power Sources **420**, 1–8 (2019). https://doi.org/10.1016/J.JPOWSOUR.2019.02.051

[23] Roberts, D., Brown, S.: Flow batteries for energy management: Novel algebraic modelling approaches to properly assess their value. Journal of Energy Storage **26** (2019). https://doi.org/10.1016/j.est.2019.100977

[24] Datasets / Climate Data Online (CDO) / National Climatic Data Centre (NCDC). https://www.ncdc.noaa.gov/cdo-web/datasets Accessed 2020-10-05